Surface wave scattering by submerged cylinders of arbitrary cross-section

R. Porter

School of Mathematics, University of Bristol, Bristol, BS8 1TW, UK.

July 3, 2001

Abstract

The reflection of surface waves normally-incident upon an infinite uniform horizontal cylinder of arbitrary cross-section totally-immersed beneath the free surface of a fluid of either finite or infinite depth is considered under the assumptions of linearised theory. The problem is formulated in terms of a first-kind integral equation for an unknown function related to the tangential velocity of the fluid around the cylinder. The kernel of the integral operator is symmetric and only weakly singular, a property that is particularly advantageous when considering thin submerged plates. Numerical results are obtained by approximating the solution using Galerkin's method and it is shown how only a few terms in the expansion are needed to gain high accuracy in the reflection and transmission coefficients. Similar accuracy is observed for thin plates where special test functions are introduced to correctly model singular behaviour at the ends of the plate. Results for both infinite and finite depth scattering are compared with existing results and new results are also presented showing zeros of transmission for families of submerged obstacle.

1 Introduction

The problem of determining the reflection of surface water waves by submerged obstacles is one of long-standing interest. The engineering benefits of using submerged bodies, rather than surface-piercing bodies exposed to violent free surface wave motions, as a means of reflecting waves make them a strong candidate for offshore breakwater devices, provided they also have the desired reflective properties.

There are few explicit solutions to the linearised water waves equations involving submerged obstacles. This is the case even when the fluid motion is two-dimensional, which is the focus of the present paper. Perhaps the most notable result is originally due to Dean (1948) who proved that a submerged horizontal circular cylinder in deep water reflects no wave energy irrespective of its radius, depth of submergence or the frequency of wave motion. This result has been subsequently reproduced by a number of authors. Ursell (1950) was the first to construct the full solution using a multipole method and his method was extended by Ogilvie (1963) who also computed first-order and second-order forces on fixed and oscillating cylinders. Also in deep water, Dean (1945) and Evans (1970) have provided closed form expressions for the reflection coefficient when waves are normally incident on thin vertical barriers extending from a point below the free surface to infinite depth and a submerged barrier of finite length respectively. For obstacles submerged in water of constant depth, no explicit expressions for the reflection coefficient are available, although powerful techniques exist for solving problems involving certain 'simple' geometries, such as thin vertical and horizontal plates, rectangular blocks and circular cylinders, where coordinate-aligned boundaries lend themselves to eigenfunction expansions and so-called multipole methods. See, for example, Porter & Evans (1995), Fernyhough (1994), Mei & Black (1966) and Ursell (1950) for scattering by a selection of such obstacles.

With the likelihood of finding analytic expressions for reflection and transmission coefficients for submerged obstacles of arbitrary cross-section remote, several methods have been devised to make some analytical progress. Thus, approximations to wave scattering by submerged obstacles of arbitrary cross-section have been made by Leppington & Siew (1980) and Grue & Palm (1984) for cylinders submerged sufficiently far below the free surface in deep water. There has also been work on 'small' cylinders that are not necessarily deeply submerged; see, for example, Davies & Leppington (1985) However, the obvious starting point from which substantial analytic headway can be achieved is by making use of Green's identity with the unknown complex velocity potential and an appropriately defined Green's function, which moves the problem onto various boundaries of the domain and thus immediately reduces the dimension of the problem. The standard approach is to use Green's identity to obtain a second-kind integral equation of the Fredholm type for the unknown potential on the cylinder surface. In this case, the kernel of the integral operator is just the derivative of the Green's function in a direction normal to the cylinder surface, which is, in general, non-singular. For a description of this method, see Vada (1987) who also extended the Green's function integral equation approach to consideration of the second-order potential. A variant of this approach is to express the potential in terms of a distribution of sources over the body, which gives a similar integral equation to solve in terms of an unknown source strength. It is equally valid to express the potential in terms of a distribution of vortices over the body subject to the constraint that there is no circulation around the body. Grue & Palm (1984) adopted this latter approach, developing ideas originally due to Wehausen & Laitone (1960), to investigate the reflection of waves from a variety of submerged obstacles. The unknown function in this case is related to the tangential velocity around the cylinder body and two integral equations are readily derived, one of the first kind involving a Cauchy-singular kernel, and another of the second kind involving a non-singular kernel. Thus, Grue & Palm (1984) also confirmed Dean's (1948) result that a circular cylinder reflected no wave energy and provided approximations to reflection and transmission coefficients for thin submerged horizontal plates and thin elliptical cylinders under the assumption that the cylinders are deeply submerged. However, they only produced very limited numerical results for a circular cylinder in infinite depth.

The approaches described in the previous paragraph all suffer when the cylinder is reduced in cross-section and replaced by a thin plate. In this case, the kernels of the various integral operators become singular and are much less suited to subsequent numerical computations. A method aimed specifically at scattering of waves by thin plates which are either totally submerged or intersect the free surface on deep water has been developed by Parsons & Martin (1992, 1994). Their approach makes initial use of Green's identity and subsequent developments lead to the formulation of a hypersingular integral equation for an unknown jump in the potential across the plate. Although the formulation is valid for arbitrary curved plates, certain explicit calculations need to be performed for each family of obstacle. By employing an approximation which incorporates the anticipated square-root type behaviour of the unknown function at the edges of the plate, a simplified set of algebraic equations was derived involving some explicit terms and in which little numerical integration was required. Further work on submerged curved thin plates has been done by McIver & Urka (1995) using the method of multipoles.

In the present paper Green's identity is used as the basis for the formulation. We take advantage of the methods introduced in Staziker *et al.* (1997) for the scattering of waves by a finite interval of arbitrary topography joining two semi-infinite regions of equal depth and recently adapted by Porter & Porter (2000) to cope with arbitrary topography joining regions of non-equal depths. The crux of the method relies on the use of Cauchy-Riemann type relations to relate normal derivatives of certain functions to tangential derivatives of other functions. Thus an integral equation of the first kind is derived for an unknown function related to the tangential velocity on the surface of the cylinder. In the case of a thin plate, the unknown is replaced by the difference of the tangential velocities either side of the plate, whilst the kernel of the integral operator, which is symmetric and only weakly (logarithmically) singular, remains unchanged. The reflection and transmission coefficients are related to inner products of this unknown function with certain prescribed functions.

The solution to the integral equation is approximated using Galerkin's method. Thus, the unknown function is approximated by an expansion in terms of a set of functions which are chosen to ensure zero circulation about the cylinder. In the case of thin plates, appropriately weighted Chebychev polynomials are used to incorporate the anticipated singularity in the velocity at the edges of the plates. Results are compared with the few analytic results that exist and with results obtained using other techniques. It is shown that only ten terms are needed in the expansion for the unknown function to ensure 6-figure accuracy in the reflection coefficient for most cylinder cross-sections and that the numerical procedure is relatively straightforward to implement and efficient to execute.

Such high accuracy is required if a numerical technique is to be used to find examples of trapping in water waves, as is considered in the companion paper, Porter (2000). That paper is based upon the fact that there exists a class of submerged cylinder cross-section which exhibit the property of total reflection at particular discrete frequencies. Thus, particular attention is focussed at establishing results for bodies having zeros of transmission.

The outline of the paper is as follows. Although ultimately results will be given for both submerged cylinders of non-zero cross-section and thin submerged plates in fluid of both finite and infinite depth, we concentrate the development of the method of formulation and solution on the case of a cylinder of non-zero cross-section in a fluid of finite depth (in sections 2, 3 and 4). Brief references will be made throughout to the relatively simple changes required when considering thin plates. The changes required for infinite depth will be confined to section 5.

In §6, results are given for a variety of geometries. Particular attention will be given to submerged obstacles having the property of zeros of transmission and in §7 some conclusions will be drawn. The two appendices contain details of algebra connected to the numerical method and a proof of the zero reflection property of a submerged circular cylinder in infinite depth (Dean 1948).

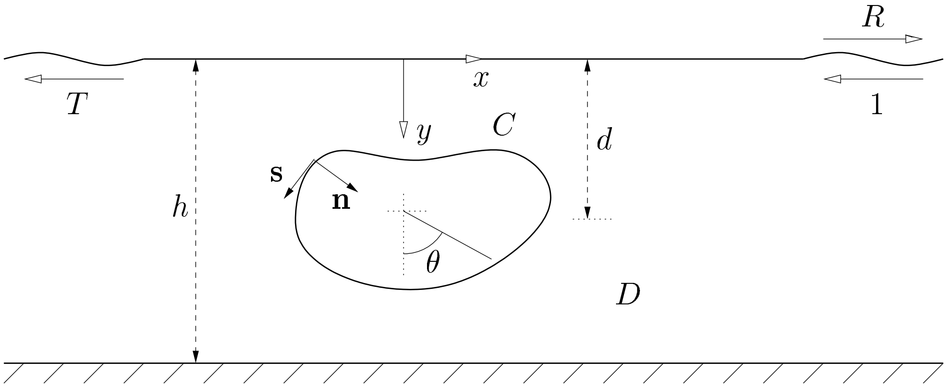

Figure 1: Description of geometry of submerged cylinder

2 Statement of problem and preliminaries

The scattering problem is two-dimensional and we choose to work with Cartesian coordinates (x, y). These are arranged so that y is measured vertically downwards, $y = 0$ coinciding with the undisturbed free surface and with the fluid bottom at $y = h$.

The cross-section of the submerged cylinder has a boundary described by the curve C, which we parametrise by writing $(x, y) = (X(\theta), Y(\theta)) \in C$, $0 \le \theta \le 2\pi$ where $\theta = 0$ is chosen to be coincident with the line $x = 0$, $y > d$ as shown in figure 1. This parametrisation allows investigation of a large class of cylinder cross-section. We shall later introduce a different parametrisation to allow thin submerged plates to be considered. The fluid occupies the region D.

According to linear water wave theory, the velocity potential Φ which describes the fluid motion can be written as

$$\Phi(x, y, t) = \Re\{\phi(x, y)\mathrm{e}^{-\mathrm{i}\omega t}\}$$

where ϕ satisfies

$$\nabla^2\phi \equiv \phi_{xx} + \phi_{yy} = 0, \qquad \text{in } D, \tag{2.1}$$

$$\phi_y + K\phi = 0, \qquad \text{on } y = 0,\ -\infty < x < \infty \tag{2.2}$$

with $K = \omega^2/g$ (g is acceleration due to gravity),

$$\phi_y = 0, \qquad \text{on } y = h \tag{2.3}$$

and

$$\phi_n = 0, \qquad \text{on } (x, y) \in C, \tag{2.4}$$

the subscript n denoting the normal derivative from D into C.

Finally, we must specify the far-field behaviour of ϕ. For a wave of unit amplitude incident from $x = \infty$,

$$\phi(x, y) \sim \begin{cases} (\mathrm{e}^{-\mathrm{i}kx} + R\mathrm{e}^{\mathrm{i}kx})\psi_0(y), & x \to \infty, \\ T\mathrm{e}^{-\mathrm{i}kx}\psi_0(y), & x \to -\infty, \end{cases} \tag{2.5}$$

where R and T are complex-valued reflection and transmission coefficients, respectively. Here, k denotes the positive real root of the usual linear dispersion relation,

$$K = k \tanh kh, \tag{2.6}$$

and later notation has been anticipated by writing

$$\left.\begin{aligned}\psi_0(y) &= N_0^{-\frac{1}{2}}\cosh k(h-y),\\ N_0 &= \tfrac{1}{2}\{1+\sinh(2kh)/2kh\},\end{aligned}\right\}. \tag{2.7}$$

The boundary-value problem for ϕ is now completely specified. We seek the solution of (2.1)–(2.5) which is continuous and infinitely differentiable everywhere in D. The principal aim of the paper is to determine R and T.

To implement the solution process described in the introduction, we require the Greens function, $G(x,y|x_0,y_0)$, in an infinite strip $-\infty < x < \infty$, $0 < y < h$, satisfying

$$\nabla^2 G = -\delta(x-x_0)\delta(y-y_0) \tag{2.8}$$

in $-\infty < x < \infty$, $0 < y < h$, where $-\infty < x_0 < \infty$, $0 < y_0 < h$, (2.2) and (2.3), and the radiation condition

$$G \sim A_{\pm}(x_0,y_0)\mathrm{e}^{\mathrm{i}k|x|}\psi_0(y), \qquad x \to \pm\infty. \tag{2.9}$$

It is a routine matter to determine G in terms of the set of eigenfunctions obtained by separation of variables in the corresponding homogeneous problem (or see Mei (1983, p.380) although his expression includes a sign error). We readily find that

$$G(x,y|x_0,y_0) = \sum_{m=0}^{\infty} \frac{\psi_m(y)\psi_m(y_0)}{2k_m h}\mathrm{e}^{-k_m|x-x_0|}, \qquad (x,y) \neq (x_0,y_0) \tag{2.10}$$

where

$$\left.\begin{aligned}\psi_m(y) &= N_m^{-\frac{1}{2}}\cos k_m(h-y),\\ N_m &= \tfrac{1}{2}\{1+\sin(2k_m h)/2k_m h\},\end{aligned}\right\} \quad m = 0,1,2,\ldots. \tag{2.11}$$

We have used k_m $(m = 1,2,\ldots)$ to denote the positive real roots of

$$K = -k_m \tan k_m h$$

arranged so that $k_m < k_{m+1}$ and we have adopted the notation $k_0 = -\mathrm{i}k$ to subsume the function $\psi_0(y)$ given in (2.7) into the definition (2.11). The set $\{\psi_m(y)\}$ is orthonormal on the interval $[0,h]$ with weight h^{-1} and it is complete.

From (2.10)

$$G \sim \frac{\mathrm{i}\psi_0(y)\psi_0(y_0)}{2kh}\mathrm{e}^{\mathrm{i}k|x-x_0|}, \qquad |x-x_0| \to \infty, \tag{2.12}$$

which implies that $A_{\pm}(x_0,y_0) = \mathrm{i}\psi_0(y_0)\mathrm{e}^{\mp \mathrm{i}kx_0}/2kh$ in (2.9).

The formulation that forms the basis of the paper uses Green's identity

$$\iint_{D'} (\phi\nabla^2 G - G\nabla^2\phi)\mathrm{d}x\mathrm{d}y = \int_{S'} \left(\phi\frac{\partial G}{\partial n} - G\frac{\partial \phi}{\partial n}\right)\mathrm{d}s, \tag{2.13}$$

where S' denotes the boundary of D', s measures the arc-length on S' and $\partial/\partial n$ is the normal derivative on S' outward from D'.

The only part of the boundary which requires particular attention is C, the curve representing the surface of the submerged cylinder. There we have, in parametric form,

$$\left.\begin{aligned}\frac{\partial}{\partial n} &= \frac{1}{\sigma(\theta)}\left(Y'(\theta)\frac{\partial}{\partial x} - X'(\theta)\frac{\partial}{\partial y}\right),\\ \frac{\partial}{\partial s} &= \frac{1}{\sigma(\theta)}\left(X'(\theta)\frac{\partial}{\partial x} + Y'(\theta)\frac{\partial}{\partial y}\right),\end{aligned}\right\} \quad 0 \le \theta < 2\pi, \tag{2.14}$$

where

$$\sigma(\theta) = \sqrt{(X'(\theta))^2 + (Y'(\theta))^2}, \qquad 0 \leq \theta < 2\pi$$

is a scaling factor. Here $\partial/\partial n$ is the inward normal derivative and $\partial/\partial s$ is the derivative along C, in the direction of increasing θ. We shall also use the (s, n) coordinates to represent a local orthogonal system in the neighbourhood of C and, in particular, apply (2.14) for points off C.

To deal with the normal derivative of a function on C, we make use of the Cauchy-Riemann equations. The functions we have to deal with, which are evident in (2.10), lead us to introduce the new (non-orthogonal) set

$$\chi_m(y) = N_m^{-\frac{1}{2}} \sin k_m(h-y), \qquad 0 \leq y \leq h, \ m = 0, 1, 2, \ldots. \tag{2.15}$$

The convention $k_0 = -\mathrm{i}k$ applies to give

$$\chi_0(y) = -\mathrm{i}N_0^{-\frac{1}{2}} \sinh k(h-y).$$

It follows easily using (2.11) and (2.14) that

$$\left.\begin{aligned} \frac{\partial}{\partial s}\psi_m(y)\mathrm{e}^{\pm k_m x} &= \mp\frac{\partial}{\partial n}\chi_m(y)\mathrm{e}^{\pm k_m x}, \\ \frac{\partial}{\partial n}\psi_m(y)\mathrm{e}^{\pm k_m x} &= \pm\frac{\partial}{\partial s}\chi_m(y)\mathrm{e}^{\pm k_m x}, \end{aligned}\right\} \qquad m = 0, 1, 2, \ldots. \tag{2.16}$$

3 Integral equation formulation

Applying (2.13) to ϕ and G on the domain $D' : \{-X < x < X, \ 0 < y < h\} \cup D$, then evaluating the limit $X \to \infty$ by means of (2.5) and (2.12), we find that

$$\phi(x_0, y_0) = \mathrm{e}^{-\mathrm{i}kx_0}\psi_0(y_0) - \int_C \phi(x, y)\frac{\partial}{\partial n}G(x, y|x_0, y_0)\mathrm{d}s, \qquad (x_0, y_0) \in D. \tag{3.1}$$

Letting $x_0 \to \infty$, using (2.5) and (2.12), we can relate the appropriate far-field coefficients to the value of ϕ on C by

$$R = -\frac{\mathrm{i}}{2kh}\int_C \phi(x, y)\frac{\partial}{\partial n}(\psi_0(y)\mathrm{e}^{-\mathrm{i}kx})\mathrm{d}s. \tag{3.2}$$

Similarly, taking the limit $x_0 \to -\infty$ in (3.1) leads to

$$T = 1 - \frac{\mathrm{i}}{2kh}\int_C \phi(x, y)\frac{\partial}{\partial n}(\psi_0(y)\mathrm{e}^{\mathrm{i}kx})\mathrm{d}s. \tag{3.3}$$

A standard procedure at this point is to move the field point (x_0, y_0) in (3.1) onto the cylinder, C, to give

$$\tfrac{1}{2}\phi(x_0, y_0) + \int_C \phi(x, y)\frac{\partial}{\partial n}G(x, y|x_0, y_0)\mathrm{d}s = \mathrm{e}^{-\mathrm{i}kx_0}\psi_0(y_0), \qquad (x_0, y_0) \in C, \tag{3.4}$$

which is the well-known boundary integral equation of the second kind for ϕ on C. Alternatively, we may operate on equation (3.1) with $\partial/\partial n_0$, the normal derivative with respect to (x_0, y_0),

$$\frac{\partial}{\partial n_0}\phi(x_0,y_0) = \frac{\partial}{\partial n_0}\left(\mathrm{e}^{-\mathrm{i}kx_0}\psi_0(y_0)\right) - \frac{\partial}{\partial n_0}\int_C \phi(x,y)\frac{\partial}{\partial n}G(x,y|x_0,y_0)\mathrm{d}s, \quad (x_0,y_0)\in D. \tag{3.5}$$

Moving the point (x_0, y_0) onto C and applying (2.4) sets the left-hand side of (3.5) to zero and results in an integral equation for the unknown potential on the cylinder. Assuming ϕ can be determined from either (3.4) or (3.5) the reflection and transmission coefficients are then given by (3.2) and (3.3). In its present form (3.5) for $(x_0, y_0) \in C$ is not well-suited to numerical computation. If one wished to make further analytic progress with (3.5) one might choose to take the normal derivative $\partial/\partial n_0$ under the integral sign. However, the resulting kernel is 'hypersingular' and the integral must be interpreted as a finite-part integral. Parsons & Martin (1992, 1994) have adopted this approach for scattering by thin flat plates and thin plates of constant curvature where the geometry was exploited to simplify certain contributions from the kernel of the integral operator. For arbitrary plates and cylinders with arbitrary non-zero cross-section, the explicit nature of the normal derivatives renders such an approach extremely complicated.

The approach in this paper uses (3.5) as its starting point but aims to replace normal derivatives with tangential derivatives using the relations (2.16), in a manner similar to that used in Porter & Porter (2000).

Thus, we note from (2.10) and (2.16) that, if $(x, y) \neq (x_0, y_0)$,

$$\frac{\partial^2}{\partial n_0 \partial n}G(x,y|x_0,y_0) = -\frac{\partial^2}{\partial s_0 \partial s}H(x,y|x_0,y_0), \tag{3.6}$$

where

$$H(x,y|x_0,y_0) = \sum_{m=0}^{\infty}\frac{\chi_m(y)\chi_m(y_0)}{2k_m h}\mathrm{e}^{-k_m|x-x_0|}. \tag{3.7}$$

Also, from the Cauchy-Riemann equations relating $\phi(x, y)$ to the streamfunction $\psi(x, y)$ it is easily confirmed using (2.14) that

$$\frac{\partial}{\partial n}\phi(x,y) = -\frac{\partial}{\partial s}\psi(x,y). \tag{3.8}$$

Using (3.6), (3.7), (3.8) and (2.16) in (3.5) gives

$$-\frac{\partial}{\partial s_0}\psi(x_0,y_0) = \frac{\partial}{\partial s_0}\left(\mathrm{e}^{-\mathrm{i}kx_0}\chi_0(y_0)\right) + \frac{\partial}{\partial s_0}\int_C \phi(x,y)\frac{\partial}{\partial s}H(x,y|x_0,y_0)\mathrm{d}s \tag{3.9}$$

Integrating the above equation with respect to s_0 and using integration by parts to transfer the tangential derivative from H to ϕ gives

$$\psi(x_0,y_0) = -\mathrm{e}^{-\mathrm{i}kx_0}\chi_0(y_0) + \int_C H(x,y|x_0,y_0)\frac{\partial}{\partial s}\phi(x,y)\mathrm{d}s, \qquad (x_0,y_0)\in D. \tag{3.10}$$

An integral equation of the first kind for $\partial\phi/\partial s$ follows by moving (x_0, y_0) onto C where the streamfunction takes a constant value ψ_C, say, so that

$$\int_C H(x,y|x_0,y_0)\frac{\partial}{\partial s}\phi(x,y)\mathrm{d}s = \mathrm{e}^{-\mathrm{i}kx_0}\chi_0(y_0) + \psi_C, \qquad (x_0,y_0)\in C. \tag{3.11}$$

At this point, we take the opportunity to introduce some new notation to deal with the parametrisation introduced at the beginning of §2, writing

$$q(\theta) = \left[X'(\theta)\frac{\partial}{\partial x} + Y'(\theta)\frac{\partial}{\partial y}\right]\phi(X(\theta), Y(\theta)), \qquad 0 \le \theta < 2\pi,$$

which is related to the tangential fluid velocity on the surface of the cylinder. We employ the shorthand notation

$$H(\theta|\theta_0) \equiv H(X(\theta), Y(\theta)|X(\theta_0), Y(\theta_0)), \qquad 0 \le \theta, \theta_0 < 2\pi,$$

and write

$$f(\theta) = \mathrm{e}^{-\mathrm{i}kX(\theta)}\chi_0(Y(\theta)), \tag{3.12}$$

such that (3.11) can be written

$$(\mathcal{K}q)(\theta_0) = f(\theta_0) + \psi_C \qquad 0 \le \theta_0 < 2\pi, \tag{3.13}$$

where

$$(\mathcal{K}q)(\theta_0) = \int_0^{2\pi} q(\theta)H(\theta|\theta_0)\mathrm{d}\theta. \tag{3.14}$$

We also introduce the inner product

$$(u, v) = \int_0^{2\pi} u(\theta)\overline{v(\theta)}\mathrm{d}\theta, \tag{3.15}$$

for functions $u, v \in L_2(0, 2\pi)$.

There are two further conditions to be imposed on the function $q(\theta)$. First, $q(\theta)$ must be continuous, i.e. $q(2\pi) = q(0)$. Secondly, the potential is continuous on C which implies

$$(q, 1) = 0. \tag{3.16}$$

Returning to equations (3.2) and (3.3), we rewrite them terms of the transferred variables

$$R = -\frac{\mathrm{i}}{2kh}\int_C \phi(x, y)\frac{\partial}{\partial s}(\chi_0(y)\mathrm{e}^{-\mathrm{i}kx})\mathrm{d}s,$$

and

$$T = 1 + \frac{\mathrm{i}}{2kh}\int_C \phi(x, y)\frac{\partial}{\partial s}(\chi_0(y)\mathrm{e}^{\mathrm{i}kx})\mathrm{d}s.$$

Integrating each of these equations by parts to switch the tangential derivative onto ϕ and employing the parametrisation in terms of θ and the definition of the inner product gives

$$R = \frac{\mathrm{i}}{2kh}(q, \overline{f_1}), \qquad \text{and} \qquad T = 1 - \frac{\mathrm{i}}{2kh}(q, f_1) \tag{3.17}$$

When the submerged obstacle is a thin plate, the curve C is given by $C = L^+ \cup L^-$, where $L^\pm$ are the two opposite sides of a line L. It is more convenient to replace our previous parametrisation by describing the curve L by $(x, y) = (X(t), Y(t)) \in L$, $-1 \le t \le 1$. The changes to the formulation are not substantial. The definition of the integral operator (3.14) is replaced by

$$(\mathcal{K}q)(t_0) = \int_{-1}^{1} q(t)H(t|t_0)\mathrm{d}t, \qquad -1 \le t_0 \le 1, \tag{3.18}$$

where

$$q(t) = \sigma(t)\{\phi_s(X(t), Y(t))|_{L^+} - \phi_s(X(t), Y(t))|_{L^-}\},$$

is now related to the jump in the tangential velocities across the plate. As before, we continue by solving (3.13) with $-1 \leq t_0 \leq 1$ and the reflection and transmission coefficients are given by (3.17) with the definition of the inner product in (3.15) replaced by

$$(u, v) = \int_{-1}^{1} u(t)\overline{v(t)}\mathrm{d}t \tag{3.19}$$

for functions $u, v \in L_2(-1, 1)$. The condition (3.16) remains unchanged. A local analysis of the velocity near the edge of the plate reveals that

$$q(t) \sim q_\pm(1 - t^2)^{-\frac{1}{2}}, \qquad \text{as } t \to \pm 1, \tag{3.20}$$

for some constants $q_\pm$.

4 Approximation and numerical procedure

The reflection and transmission coefficients are given by (3.17) where $q(\theta)$, is the solution of (3.13). A Galerkin method is chosen for approximating the solution to the integral equations, (3.13) in which we write

$$q(\theta) \approx \tilde{q}(\theta) = \sum_{n=1}^{2N} a_n u_n(\theta), \qquad 0 \leq \theta < 2\pi, \tag{4.1}$$

where a_n are a set of coefficients to be determined. The set of expansion functions, $\{u_n\}$, $n = 0, 1, \ldots$ are chosen to be real, complete in $L_2(0, 2\pi)$ and to satisfy

$$(u_n, 1) = 0, \qquad \text{n=1,2,}\ldots, \tag{4.2}$$

to ensure that the condition (3.9). The term u_0 satisfies $(u_0, 1) \neq 0$. The truncation size $2N$ in (4.1) is chosen to be even in anticipation of the choice of the set $\{u_n\}$, which are considered later. The coefficients a_n, $n = 1, \ldots, 2N$ and the constant ψ_C are determined by solving

$$(\mathcal{K}\tilde{q} - f, u_m) = 0, \qquad m = 0, 1, \ldots, 2N,$$

a process which characterises Galerkin's method. Substitution of (4.1) into the above results in the systems of equations

$$\sum_{n=1}^{2N} a_n K_{mn} = F_m, \qquad m = 1, \ldots, 2N, \tag{4.3}$$

whilst, for $m = 0$,

$$\sum_{n=1}^{2N} a_n K_{0n} = F_0 + (1, u_0)\psi_C, \tag{4.4}$$

where we have defined

$$\left.\begin{aligned} K_{mn} &= (\mathcal{K}u_n, u_m), \qquad n = 1, 2, \ldots, \quad m = 0, 1, \ldots \\ F_m &= (f, u_m), \qquad m = 0, 1, \ldots \end{aligned}\right\} \tag{4.5}$$

Finally,

$$R \approx \tilde{R} = \frac{\mathrm{i}}{2kh} \sum_{n=1}^{2N} a_n F_n \qquad T \approx \tilde{T} = 1 - \frac{\mathrm{i}}{2kh} \sum_{n=1}^{2N} a_n \overline{F_n}. \tag{4.6}$$

Thus, the coefficients a_n, $n = 1, 2, \ldots$ are determined by (4.3) whence $\tilde{R}$ and $\tilde{T}$ are given by (4.6) and ψ_C is given by (4.4).

The choice of functions, u_n, to be used in the approximation of q, in (4.1) is dependent upon the geometry of the submerged obstacle. For cylinders with non-zero cross-section, the unknown functions need to be expanded in a set of continuous 2π-periodic functions. A clear choice for smooth cylinder boundaries is the Fourier series,

$$\left.\begin{aligned} u_{2n}(\theta) &= \cos(n\theta) \\ u_{2n-1}(\theta) &= \sin(n\theta) \end{aligned}\right\}, \qquad n = 1, 2, \ldots, \quad 0 \leq \theta \leq 2\pi, \tag{4.7}$$

which satisfy (4.2) as required, whilst $u_0 = \frac{1}{2}$ such that $(u_0, 1) = \pi$.

If the submerged obstacle is a thin plate, the unknown functions to be approximated are related to the jump in tangential velocity across the plate with singular end-point behaviour given by (3.20). The set

$$u_n(t) = (1 - t^2)^{-\frac{1}{2}} T_n(t), \qquad n = 0, 1, \ldots, \quad -1 < t < 1, \tag{4.8}$$

is chosen, where $T_n(x)$ is the orthogonal Chebychev polynomial. Again, (4.2) is satisfied by this choice, whilst $(u_0, 1) = \pi$. This latter set of functions has been used extensively for approximating solutions to potential flow problems involving thin plates. See, for example, Porter & Evans (1995) where Chebychev polynomials were used with success in a related problem.

In both of the cases above u_n are even and odd functions for even and odd values of n respectively which is why the truncation size in (4.1) is chosen to be even so that no bias is given towards either the even or odd component of the solution.

Numerical issues

The only terms requiring particular attention when it comes to numerical computation are the matrix elements K_{mn}. We first write

$$K_{mn} = K_{mn}^{(w)} + K_{mn}^{(e)}, \qquad m, n = 1, \ldots, 2N$$

the superscripts (w) and (e) used to denote the division between wave-like and evanescent contributions to the Green's function, such that

$$K_{mn}^{(w)} = \frac{\mathrm{i}}{2kh} \int_0^{2\pi} u_m(\theta_0) \chi_0(Y(\theta_0)) \int_0^{2\pi} u_n(\theta) \chi_0(Y(\theta)) \mathrm{e}^{\mathrm{i}k|X(\theta) - X(\theta_0)|} \mathrm{d}\theta \mathrm{d}\theta_0, \tag{4.9}$$

and

$$K_{mn}^{(e)} = \int_0^{2\pi} u_m(\theta_0) \int_0^{2\pi} u_n(\theta) \sum_{r=1}^{\infty} \frac{\chi_r(Y(\theta)) \chi_r(Y(\theta_0))}{2k_r h} \mathrm{e}^{-k_r|X(\theta) - X(\theta_0)|} \mathrm{d}\theta \mathrm{d}\theta_0. \tag{4.10}$$

There is no difficulty computating $K_{mn}^{(w)}$. However, numerical evaluation of $K_{mn}^{(e)}$ requires careful attention since the kernel of the double integral in (4.10) is inseparable and logarithmic singular. Appendix A describes how $K_{mn}^{(e)}$ can be written as the sum of three terms,

$$K_{mn}^{(e)} = K_{mn}^{(1)} + K_{mn}^{(2)} + K_{mn}^{(3)},$$

defined by (A.3), (A.7) and (A.8) respectively, each of which is suitable for numerical computation.

For thin plates, there is only a slight difference connected with the change in parametrisation of the submerged obstacle, already detailed in §3. Also note the comments at the end of Appendix A with regards to computing the terms $K_{mn}^{(2)}$ and $K_{mn}^{(3)}$ for thin plates.

Finally, we comment that conservation of energy, which requires that $|R|^2 + |T|^2 = 1$, is automatically satisfied by any approximation to the exact solution of the problem as a consequence of the formulation that has been employed. This can be shown by taking the limits $x_0 \to \pm\infty$ in (3.1) and substituting the approximation $\tilde{q}$ in place of q. The resulting approximation $\tilde{\phi}$ to ϕ can then be shown to satisfy

$$\tilde{\phi}(x, y) \sim \begin{cases} (\mathrm{e}^{-\mathrm{i}kx} + \tilde{R}\mathrm{e}^{\mathrm{i}kx})\psi_0(y), & x \to \infty, \\ \tilde{T}\mathrm{e}^{-\mathrm{i}kx}\psi_0(y), & x \to -\infty. \end{cases}$$

Using $\tilde{\phi}$ and its complex conjugate as the two functions in Green's identity (2.13), shows that $|\tilde{R}|^2 + |\tilde{T}|^2 = 1$.

5 Infinite depth

When the fluid is of infinite depth there is no fundamental difference to the approach used for finite depth, and details of the changes required will be outlined briefly now. Thus, instead of (2.3), the condition for large depths is

$$\nabla\phi \to 0, \qquad \text{as } y \to \infty,$$

whilst the dispersion relation (2.6) is just $k = K$ in deep water and (2.5) is replaced by

$$\phi(x, y) \sim \begin{cases} (\mathrm{e}^{-\mathrm{i}Kx} + R\mathrm{e}^{\mathrm{i}Kx})\mathrm{e}^{-Ky}, & x \to \infty, \\ T\mathrm{e}^{-\mathrm{i}Kx}\mathrm{e}^{-Ky}, & x \to -\infty. \end{cases}$$

The two-dimensional Greens function for a submerged line source in infinite depth can be found in, for example, Wehausen & Laitone (1960) and in the present notation is written as

$$G_\infty(x, y|x_0, y_0) = -\frac{1}{2\pi}\ln\left(\frac{r_0}{r_1}\right) - \frac{1}{\pi}\int_0^\infty \frac{\mathrm{e}^{-\nu(y+y_0)}}{K - \nu}\cos\nu(x - x_0)\mathrm{d}\nu + \mathrm{i}\mathrm{e}^{-K(y+y_0)}\cos K(x - x_0),$$

where the integral is Cauchy principal-valued and

$$r_0^2 = (x - x_0)^2 + (y - y_0)^2, \qquad r_1^2 = (x - x_0)^2 + (y + y_0)^2. \tag{5.1}$$

The far-field behavior of the Green's function is

$$G_\infty(x, y|x_0, y_0) \sim \mathrm{i}\mathrm{e}^{-K(y+y_0)}\mathrm{e}^{\mathrm{i}K|x-x_0|}, \qquad |x - x_0| \to \infty.$$

In order to implement our method, certain Cauchy-Riemann type relations are needed. For example,

$$\frac{\partial}{\partial s}(\mathrm{e}^{-Ky\pm\mathrm{i}Kx}) = \mp\frac{\partial}{\partial n}(-\mathrm{i}\mathrm{e}^{-Ky\pm\mathrm{i}Kx})$$

amongst others (these are just (2.16) with $m = 0$). Thus, it is not difficult to confirm that

$$\frac{\partial^2}{\partial n_0 \partial n} G_\infty(x, y|x_0, y_0) = -\frac{\partial^2}{\partial s_0 \partial s} H_\infty(x, y|x_0, y_0), \tag{5.2}$$

where

$$\begin{aligned} H_\infty(x, y|x_0, y_0) &= -\frac{1}{2\pi}\ln(r_0 r_1) + \frac{1}{\pi}\,⨍_0^\infty \frac{\mathrm{e}^{-\nu(y+y_0)}}{K-\nu}\cos\nu(x-x_0)\mathrm{d}\nu - \mathrm{i}\mathrm{e}^{-K(y+y_0)}\cos K(x-x_0) \\ &\equiv H_\infty^{(s)} + H_\infty^{(r)} + H_\infty^{(i)}. \end{aligned} \tag{5.3}$$

The function $H_\infty(x, y|x_0, y_0)$ is equivalent to the streamfunction due to a pulsating line vortex at $(x, y) = (x_0, y_0)$ (see, for example, Wehausen & Laitone (1960)). Yu & Ursell (1961) showed that the principal value integral defining the middle term, $H_\infty^{(r)}$, in (5.3), could be written in a form more suitable for computation as

$$\begin{aligned} H_\infty^{(r)}(x, y|x_0, y_0) &= \mathrm{e}^{-K(y+y_0)}\Big((\gamma + \ln(Kr_1))\cos K(x-x_0) + \theta_1 \sin K(x-x_0)\Big)/\pi \\ &\quad -\frac{1}{\pi}\sum_{m=1}^{\infty}\frac{(-Kr_1)^m}{m!}\left(1+\frac{1}{2}+\ldots+\frac{1}{m}\right)\cos m\theta_1, \end{aligned} \tag{5.4}$$

where $\gamma = 0.5772...$ is Euler's constant and $\theta_1 = \tan^{-1}[(x-x_0)/(y+y_0)]$.

Apart from the different representation for the Green's function, the formulation in infinite depth follows that already described for finite depth. Thus, application of Green's identity in infinite depth gives the equations

$$\phi(x_0, y_0) = \mathrm{e}^{-Ky_0-\mathrm{i}Kx_0} - \int_C \phi(x, y)\frac{\partial}{\partial n}G_\infty(x, y|x_0, y_0)\mathrm{d}s, \qquad (x_0, y_0) \in D,$$

with

$$R = -\mathrm{i}\int_C \phi(x, y)\frac{\partial}{\partial n}(\mathrm{e}^{-Ky-\mathrm{i}Kx})\mathrm{d}s \tag{5.5}$$

and

$$T = 1 - \mathrm{i}\int_C \phi(x, y)\frac{\partial}{\partial n}(\mathrm{e}^{-Ky+\mathrm{i}Kx})\mathrm{d}s. \tag{5.6}$$

Following the formulation described in §3 for finite depth results in an integral equation of the form (3.13), but with the kernel of the integral operator replaced by $H_\infty(\theta|\theta_0) = H_\infty(X(\theta), Y(\theta)|X(\theta_0), Y(\theta_0))$ as defined by (5.3), and with

$$f(\theta) = \mathrm{i}\mathrm{e}^{-KY(\theta)-\mathrm{i}KX(\theta)},$$

replacing (3.12).

Notice also the factor of $1/(2kh)$ multiplying the integrals in (3.2) and (3.3) in the finite depth case but missing from the expressions for R and T in (5.5) and (5.6) above. Hence this factor must also be omitted from (3.17) and (4.6) to obtain expressions for R and T appropriate to the infinite depth case.

The Galerkin approximation is applied in an identical manner to that described in §4. The only changes are from the altered definitions of the kernel of the integral equation. Thus we write

$$K_{mn} = K_{mn}^{(s)} + K_{mn}^{(r)} + K_{mn}^{(i)}, \qquad m,n = 1,\ldots,2N,$$

where

$$K_{mn}^{(s,r,i)} = \int_0^{2\pi} u_m(\theta_0) \int_0^{2\pi} u_n(\theta) H_\infty^{(s,r,i)}(\theta|\theta_0) \mathrm{d}\theta \mathrm{d}\theta_0. \tag{5.7}$$

Here, the only term needing particular attention is $K_{mn}^{(s)}$ which is logarithmically singular and not suitable for numerical evaluation in its present form. In Appendix A, it is shown that $K_{mn}^{(s)}$ can be written as the sum of two terms $K_{mn}^{(2)}$ and $K_{mn}^{(3)}$ defined by (A.7) and (A.8) respectively and with $T(\theta,\theta_0) = r_0 r_1$, defined by (5.1), which allows efficient and accurate numerical computations can be made.

6 Results

The submerged obstacles for which results are produced in this paper are: elliptical cylinders (including circular cylinders) of width $2a$ and height $2b$ with centre submerged to a depth d; thin flat plates of width $2a$ inclined at an angle δ to the horizontal with the uppermost point submerged to a depth d; and thin symmetrical circular curved plates of arc length $2a$ subtending an angle 2δ with the uppermost part of the arc submerged to a depth d. They are described parametrically as follows:

$$\left.\begin{array}{ll} \text{(i) elliptical cylinder:} & X(\theta) = a\sin\theta,\ Y(\theta) = d + b\cos\theta, \\ \text{(ii) flat inclined plate:} & X(t) = at\cos\delta,\ Y(t) = d + a(1-t)\sin\delta, \\ \text{(iii) curved plate:} & X(t) = a\sin(\delta t)/\delta,\ Y(t) = d + a(1-\cos(\delta t))/\delta, \end{array}\right\} \tag{6.1}$$

The first task is to assess the accuracy and efficiency of the method presented in this paper. The accuracy of the results will be crucial in demonstrating trapped wave results in the companion paper, Porter (2001). We have already established at the end of §4 that conservation of energy is satisfied automatically as a consequence of the formulation and cannot be used to assess the accuracy of the approximation.

In Table 1 we present results showing the convergence of $|R|$ with truncation size $2N$ for four contrasting examples which have been chosen to demonstrate the success of the method in extreme geometrical cases.

In the first column of table 1 numerical results are compared with the exact result due to Evans (1970) for the scattering by a thin vertical plate in deep water. Since the obstacle is a thin plate, the test functions used in the expansion are those given in (4.8) that incorporate the inverse square-root singularity. It can be seen that the convergence in this extreme case where the top edge of the plate is very close to the free surface is excellent with 6-figure agreement to the exact result having being achieved with just 8 terms in the expansion. Convergence improves with increasing depth of submergence of the top of the plate.

In the middle two columns of table 1 we examine the convergence of a very thin elliptical cylinder ($b/a = 0.02$) and compare with the results for a thin horizontal plate of the same

2N	Vertical Plate ($a/d = 10$, $Ka = 1$)	Thin elliptical cylinder ($a/d = 5$, $Ka = 1.5$) ($b/a = 0.02$)	($b/a = 0$)	Circular cylinder ($a/d = 0.95$, $Ka = 1$
2	0.517659	0.853382	0.446101	0.000000
4	0.527695	0.473303	0.362595	0.000000
6	0.527817	0.282115	0.356740	
8	0.527820	0.395552	0.356690	
10		0.386102	0.356690	
12		0.388058		
14		0.387958		
16		0.387961		
Exact result	0.527820 Evans (1970)	-	-	0 Dean (1948)

Table 1: Convergence of $|R|$ with trunction size $2N$ for submerged obstacles in deep water.

width. The left-hand column demonstrates the effectiveness of a Fourier series approximation to the tangential velocity even when the cylinder boundary includes regions of very high curvature where large localised tangential velocities are to be expected. In contrast, when the cylinder is reduced to a thin plate and the test functions used are given by (4.8), incorporating the singular behaviour at the end points of the plate, the method converges rapidly as shown in the right-hand middle column.

The final column of table 1 shows the computed numerical approximations to $|R|$ for a submerged circular cylinder in deep water, which Dean (1948) showed is precisely zero for all values of cylinder radius and wave frequency. Here, the numerical results appear to show $\tilde{R}$ is identically zero for all N. This result is proved in Appendix B, from which it also follows that $R = 0$, yet again confirming Dean's (1948).

Computational speed is not heavily dictated by the truncation size, $2N$, (providing N is not excessively large) and we have chosen a value of $N = 8$ for producing all the curves that follow. The majority of the computational effort goes into calculating the symmetric matrix of elements K_{mn}. The decomposition of K_{mn} into several components designed to increase the accuracy and efficiency of numerical computations has been described in §4 for the finite depth case and at the end of §5 for infinite depth. In the computation of the components of K_{mn}, and the right-hand side terms F_n, integrals need to evaluated numerically. For this, a 10-point Guass-Legendre quadrature is used, each integral requiring 100 evaluations of the integrand to obtain a desired accuracy of 8 decimal places. This accuracy is sufficient to then claim 6-figure accuracy in the reflection and transmission coefficients.

In figure 2 we show the effect of finite depth upon the reflection coefficient for a submerged circular cylinder. In infinite depth, $R = 0$ (Dean 1948) for all frequencies, but as the fluid bottom is raised from the depths there is, on average, increased reflection over all frequencies. Indeed, increase in reflection as the depth of fluid is reduced is a general result, regardless of the cylinder cross-section. In figure 2, the depth of submergence of the centre of the cylinder is chosen to be $a/d = 0.9$ and curves are shown for non-dimensional depths given by $d/h = 0.1, 0.2, 0.4$. The non-dimensional quantity Ka has been used as the measure of variation of $|R|$ with frequency, where $K = \omega^2/g$ is related to the radian frequency of motion

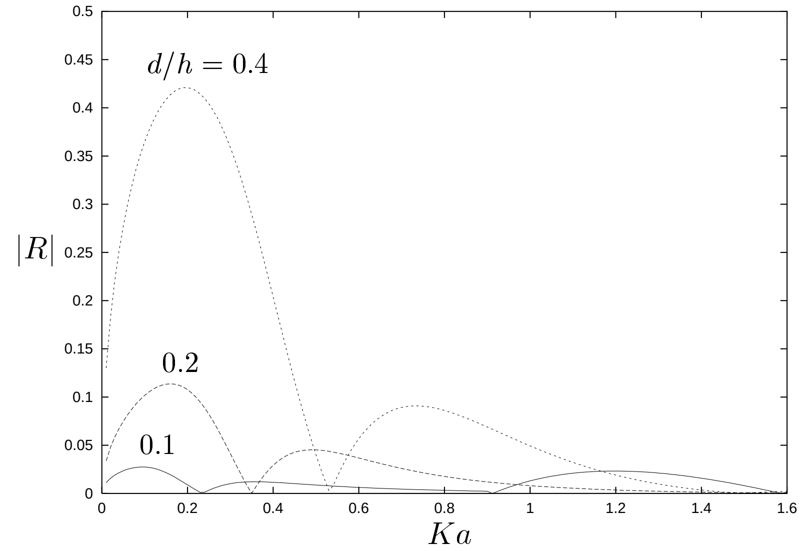

Figure 2: Variation of $|R|$ with Ka for a circular cylinder, $a/d = 0.9$, in fluid of finite depth h (d/h shown against curves).

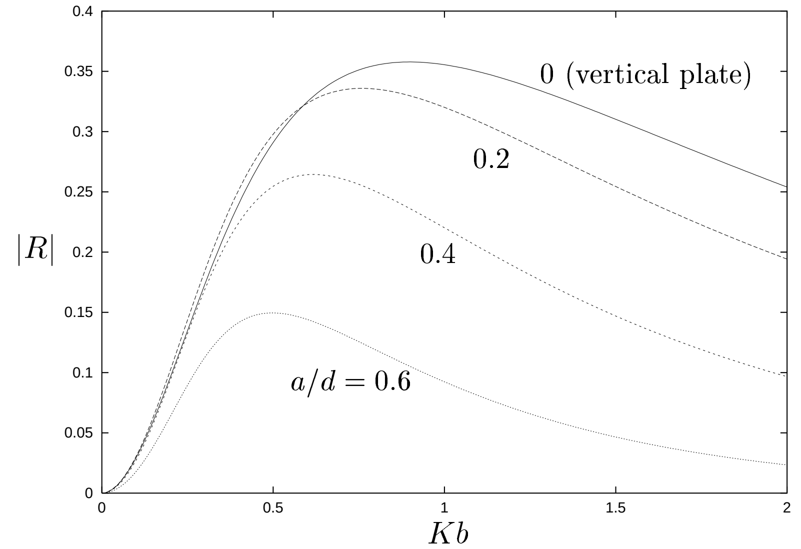

Figure 3: Variation of $|R|$ with Kb for elliptical cylinders with constant $b/d = 0.8$ in deep water and for various a/d (shown against curves).

and $2a$ is the characteristic width of the submerged obstacle – see (6.1).

The occurrence of frequencies at which $R = 0$ as seen in figure 2 is common in the scattering of surface waves by submerged obstacles and/or topography (see, for example, Newman (1966)).

In figure 3 is shown the variation of modulus of reflection coefficient with Kb for a family of elliptical cross-section cylinders in fluid of infinite depth. Here, we have fixed the height of the cylinder with respect to the depth with $b/d = 0.8$ and varied the width of the cylinder by choosing $a/d = 0, 0.2, 0.4, 0.6$. For a value of $a/d = 0.8$, the ellipse reduces to a circle and $R = 0$. For $a/d = 0$, we just have the case of a thin vertical plate for which the expansion functions (4.8) are used. This curve for $a/d = 0$ could have equally been computed using the analytic expression given in Evans (1970). The results in figure 3 are not particularly

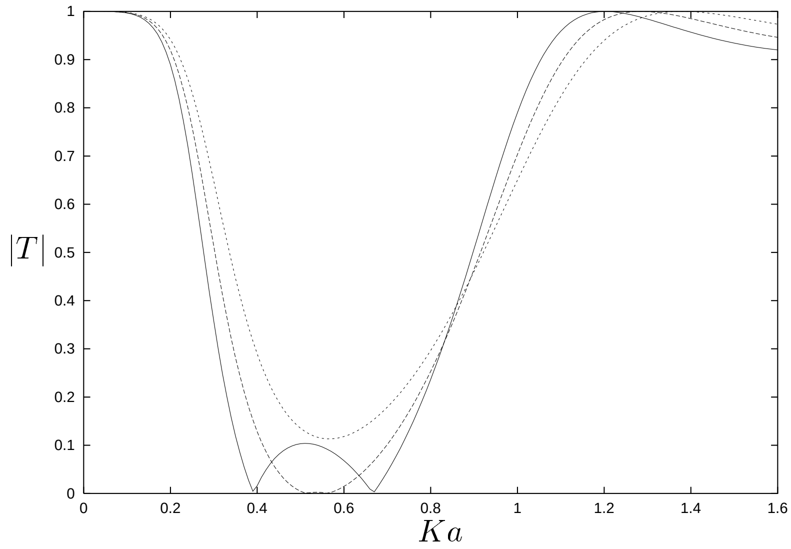

Figure 4: Variation of $|T|$ with Ka for a thin horizontal plate for different widths in deep water: $a/d = 5$(—), 4.5(- - -), 4($\cdots$).

surprising, and show that the thin vertical plate exhibits the largest reflection on average over the range of frequencies, with reduced reflection from 'rounder' bodies.

Figure 4 shows the variation $|T|$ with Ka for a thin horizontal ($\delta = 0$) submerged plate for the three non-dimensional plate widths $a/d = 4, 4.5, 5$ in an infinite depth fluid. It can be seen that for the longest plate, $a/d = 5$, there are clearly two frequencies at which $|T| = 0$, whilst the same is also true for a slightly shorter plate $a/d = 4.5$, although this is not quite so easy to observe from the figure. As the width of the plate is reduced still further the zero of transmission is lost as can be seen for the curve with $a/d = 4$. The occurrence of frequencies at which total reflection occurs for a submerged horizontal plate is not a new result and similar figures have been presented, for example, in Parsons & Martin (1992). Results for thin submerged horizontal plates in finite depth water also exist and can be found in, for example, Pataranich (1984), McIver (1985) and Fernyhough (1994) using a variety of techniques that lend themselves to the particular geometry in question.

The occurrence of zeros of transmission for long submerged thin horizontal plates is an interesting phenomenon and it is natural to ask what other submerged bodies also exhibit zeros of transmission and what effect the depth has on their existence. Thus, in figure 5 we show curves of values of Ka with varying plate width, a/d, at which zeros of transmission occur for elliptical cross-sections ranging from $b/a = 0$ (a flat horizontal plate) to $b/a = 0.16$ in fluid of infinite depth. This upper limit of $b/a = 0.16$ was chosen since an elliptical cylinder of aspect ratio $b/a = 0.2$ intersects the free surface at $a/d = 5$. However, larger values of b/a can be considered providing a/d is low enough to ensure the cylinder is submerged. Of course, it is known that zeros of transmission cannot exist for the aspect ratio $b/a = 1$, since this is the circular cylinder for which $|T| = 1$ for all Ka, so there must be some critical ratio of b/a above which zeros of transmission cease to exist. Numerical experimentation shows that this value is $b/a \approx 0.57$ with $a/d \approx 1.75$ such that the cylinder is barely submerged.

In figure 6 and 7 we investigate the effect of the fluid depth on the existence of zeros of transmission. Firstly, in figure 6 we take a thin horizontal plate of fixed width $a/d = 10$ and present curves for non-dimensional depths $d/h = 0, 0.1, 0.2, 0.4$. The curve labelled $d/h = 0$ corresponds to infinite depth and is identical to the curve labelled $\delta = 0$ in figure 5 of Parsons

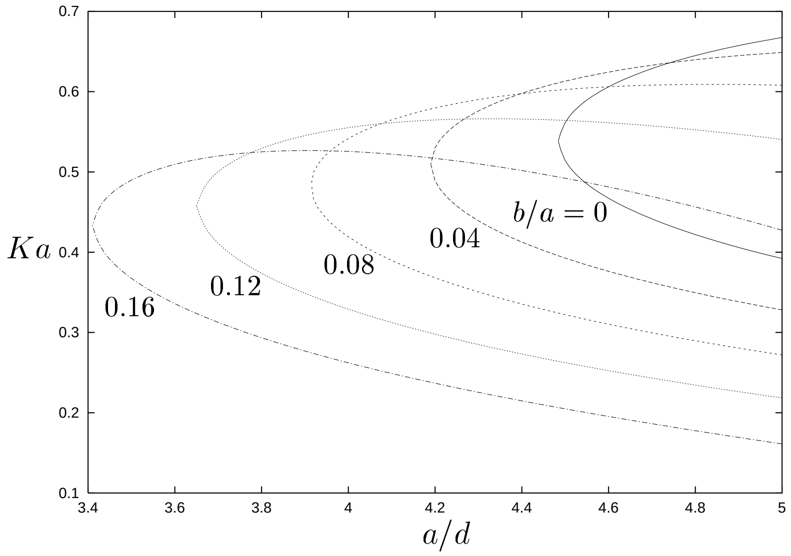

Figure 5: Values of Ka for which $T = 0$ as the non-dimensional width of an ellipse, a/d, is varied in deep water. The aspect ratio of the ellipses, b/a, is shown against curves.

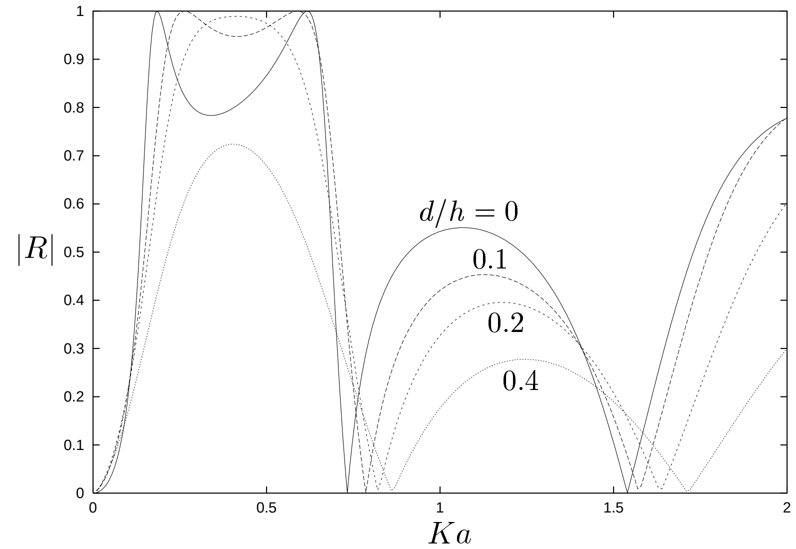

Figure 6: Variation of $|R|$ with Ka for a thin horizontal plate of width $a/d = 10$ water of finite depth h (d/h shown against curves).

& Martin (1992). It can be seen from figure 6 that there exist frequencies at which $|R| = 1$ provided the fluid is sufficiently deep ($d/h = 0, 0.1$) which disappear as d/h is increased (the depth of fluid is reduced).

Figure 7 is similar to 5 and traces the frequencies at which zeros of transmission occur as d/h is varied for ellipses of equal width $a/d = 5$ and with aspect ratios, $b/a = 0, 0.08, 0.16$. These range from to a thin flat horizontal plate to an ellipse which is close to the free surface ($b/d = 0.8$). From figure 5, it is known that zeros of transmission exist for all three ellipses in infinite depth and these values are marked by points on the ordinate $d/h = 0$ in figure 7. The finite depth calculations are performed for $d/h \geq 0.005$. Figure 7 reinforces the results seen in figure 6 and shows that the fluid depth has a significant effect upon the existence of zeros of transmission which rapidly disappear as the depth of the fluid is reduced (i.e. d/h

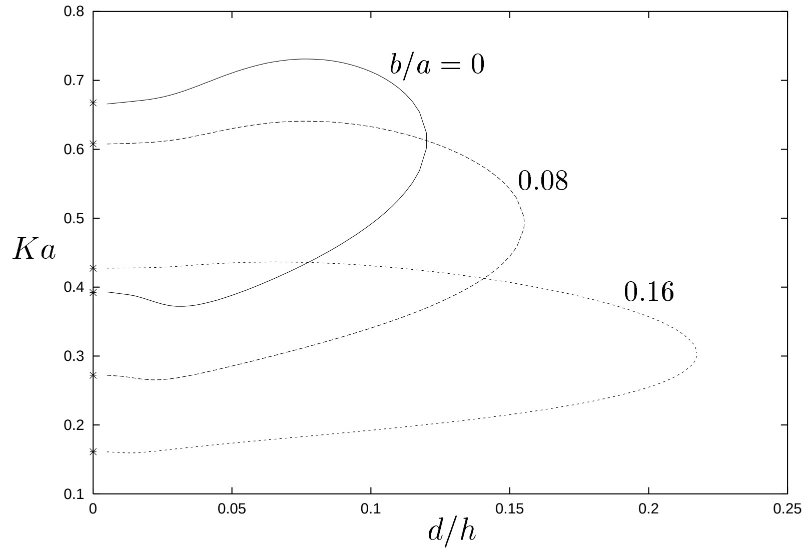

Figure 7: Values of Ka for which $T = 0$ as the non-dimensional fluid depth, d/h is varied for ellipses with $a/d = 5$ and for aspect ratios, b/a, shown against curves.

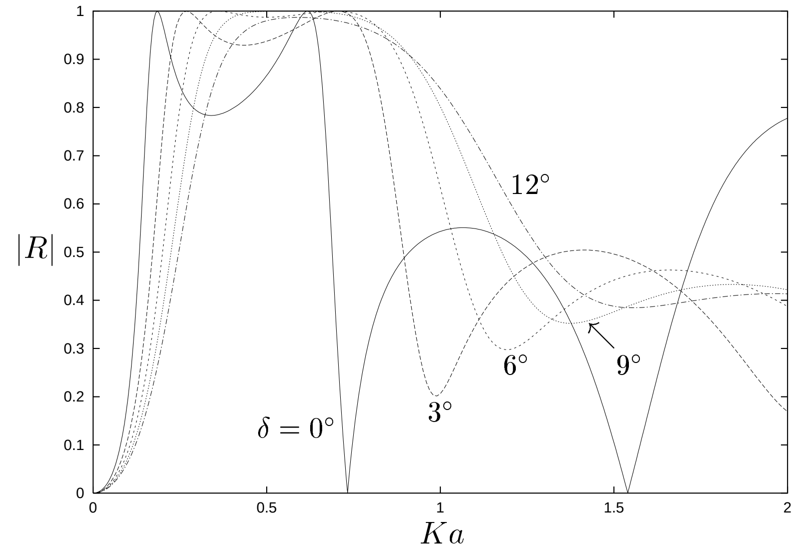

Figure 8: Variation of $|R|$ with Ka for a thin plate with $a/d = 10$ in deep water inclined at an angle δ (shown against the curves).

increasing from zero). As already seen in figure 5, it is the thin plate $b/a = 0$ whose zeros of transmission are most sensitive to parameters, whilst for larger aspect ratio ellipses, zeros of transmission exist over a broader range of parameters.

Having investigated the effect of finite depth and the broadening of the horizontal plate into a thin elliptical cylinder on the existence of zeros of transmission, we now examine the effect of increasing the angle of inclination, δ, of the plate from the horizontal ($\delta = 0°$). In figure 8 we choose a thin flat plate of width $a/d = 10$ in deep water so that the curve for $\delta = 0°$ is identical to that already presented in figure 6 for $d/h = 0$. In figure 8 variation of $|R|$ with Ka is shown for inclination angles of $\delta = 0°, 3°, 6°, 9°, 12°$. The curve for $\delta = 9°$ is identical to the curve labelled 0.1 in figure 4 of Parsons & Martin (1992). It can be seen that as the angle of inclination is increased, the zeros of transmission eventually disappear.

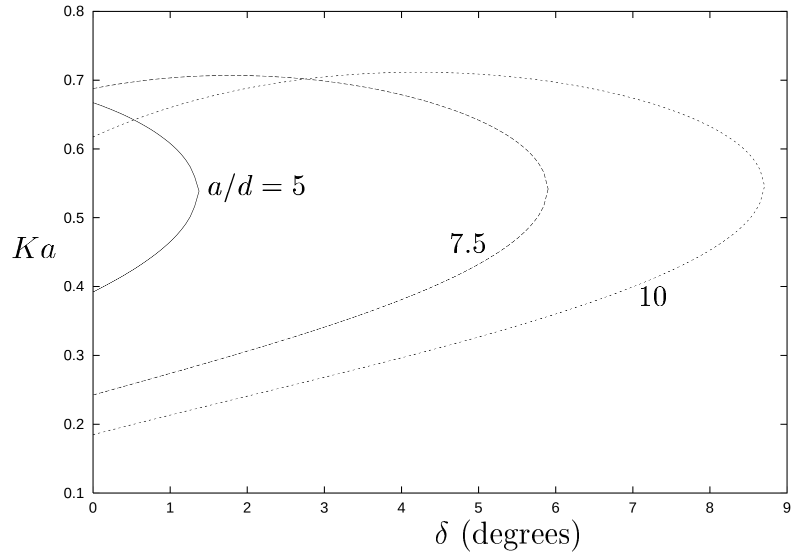

Figure 9: Values of Ka for which $T = 0$ as the angle of inclination, δ is varied a thin flat plate in deep water of width a/d (shown against curves).

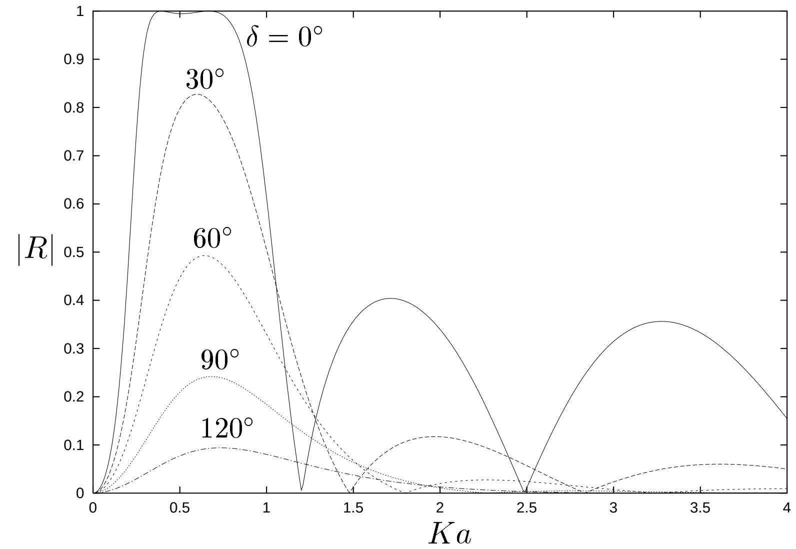

Figure 10: Variation of $|R|$ with Ka for a thin downward-curving plate with $a/d = 5$ in deep water and for curvatures, δ, shown against the curves.

This is shown more clearly in figure 9 where curves showing dependence of frequencies for which $T = 0$ upon angle δ are sketched for flat plates of width $a/d = 5, 7.5, 10$. Thus, a plate of width $a/d = 5$ cannot be rotated further than approximately $1.5°$ about one end before zeros of transmission are lost. As the plate width is increased, zeros of transmission can be seen to persist for larger values of δ.

Finally, we investigate the effect of curvature of a thin plate upon the reflection coefficient in figure 10 for a circular plate curving downwards (away from the free surface) from the horizontal. The description of this plate is given in (6.1) such that the d represents the distance of the top of the plate from the free surface whilst the arc-length of the curved circular plate is $2a$. Again, we use $a/d = 5$ and $\delta = 0°$ as the reference curve in figure 10 which we have already shown has two frequencies at which $|R| = 1$. As the curvature δ

is increased from zero, then the zeros of transmission persist, although only for small δ as already observed in the case of a thin flat inclined plate. Thus, rather than focussing on zeros of transmission, we present curves for much larger increments in δ of $30°$ in figure 10. The reflection coefficient rapidly decreases from a maximum of unity for the flat plate. This is because the waves are most affected by the shape of the submerged obstacle nearest to the free surface, which soon resembles a circular cylinder as δ increases. Also see McIver & Urka (1995) who considered the same problem using the method of multipoles. As $\delta \to 180°$ corresponding to closing the plate into a circle, the reflection coefficient inevitably tends to zero.

7 Conclusions

In this paper a new approach to determining the reflection of small-amplitude time-harmonic water waves from fixed submerged horizontal cylinders of arbitrary cross-section has been derived in which the reflection and transmission coefficients are given in terms of the solution to an integral equation with a symmetric kernel which is only weakly singular. The advantage of the present method over previous approaches to this problem lies in the ease of computation of the kernel of the integral operator which does not suffer when thin submerged plates are considered. The approximation to the integral equation is performed using a Galerkin scheme in which the unknown function is expanded in a set of functions which are chosen to satisfy certain properties of the solution.

Scattering in both finite and infinite depth has been considered and a large class of submerged obstacle has been studied, including inclined and curved thin plates. The zero reflection property discovered by Dean (1948) for a submerged circular cylinder in infinite depth is satisfied exactly by the approximation employed. Moreover, this has been shown to be because the method of formulation coupled with a Galerkin approximation results in exactly the system of equations derived by Ursell (1950) using a multipole method designed specifically for problems involving submerged circular cylinders. Although no details have been presented in this paper, the present approach, when applied to thin vertical plates, results in a system of equations closely resembling those in Porter & Evans (1995) who derived 'complementary' methods designed specifically for accurately and efficiently predicting approximations to wave scattering by thin vertical plates. In fact, it can be shown that the present method applied to the submerged vertical barrier gives rise to a further two 'complementary' formulations, derived in the same manner as those in Porter & Evans (1995), but with the problem posed initially in terms of the streamfunction as opposed to the velocity potential.

Since the present method which is based on arbitrary submerged obstacles reduces in two contrasting special cases – the cylinder and the vertical plate – to highly effective methods specifically designed for solving those problems it is perhaps not surprising that efficient and accurate results are also produced for the whole range of geometries studied in the present paper. This accuracy is crucial if one is interested in numerically determining trapped waves solutions, as is done in Porter (2001).

The obvious limitation of the approach presented in this paper is that it is not clear how it can be extended to three-dimensional scattering since it relies on the use of the Cauchy-Riemann equations. Further, it is not clear yet how the method can be adapted for cylinders of arbitrary cross-section piercing the free surface. This is because additional terms would result from the step involving integration by parts in the derivation of the integral equation due to the fact that the integration is not over a closed boundary.

Appendix A. Calculation of K_{mn}

In the case of finite depth the double integral defining $K_{mn}^{(e)}$ in (4.10) is not in a suitable form for computation, the difficulty lying in the presence of a logarithmic singularity in the inseparable kernel of the double integral. The first part of this Appendix shows how the logarithmic singularity is extracted from this kernel. In infinite depth the logarithmic singularity is already exposed in the factor defined by $K_{mn}^{(s)}$. Later on in the Appendix, we describe how logarithmic singularities are treated in order to make accurate numerical calculations possible.

We comment on the alterations required for the flat plate at the end of the Appendix, concentrating on the case of a cylinder with non-zero cross-section.

Note first the leading order asymptotic behaviour of k_r is given by $k_r \sim r\pi/h$ whence $N_r \sim \frac{1}{2}$ and $r \to \infty$ and so

$$\chi_r(Y(\theta)) \sim \widehat{\chi}_r(Y(\theta)) = \sqrt{2}\sin\{r\pi(1 - Y(\theta)/h)\}, \qquad \text{as } r \to \infty.$$

We re-write the infinite sum in the kernel of the double integral in (4.10) as

$$\sum_{r=1}^{\infty} \frac{\chi_r(Y(\theta))\chi_r(Y(\theta_0))}{2k_r h} \mathrm{e}^{-k_r|X(\theta)-X(\theta_0)|} = S(\theta,\theta_0) + \frac{1}{2\pi}\ln T(\theta,\theta_0) \tag{A.1}$$

where

$$S(\theta,\theta_0) = \sum_{r=1}^{\infty}\left[\frac{\chi_r(Y(\theta))\chi_r(Y(\theta_0))}{2k_r h}\mathrm{e}^{-k_r|X(\theta)-X(\theta_0)|} - \frac{\widehat{\chi}_r(Y(\theta))\widehat{\chi}_r(Y(\theta_0))}{2r\pi}\mathrm{e}^{-r\pi|X(\theta)-X(\theta_0)|/h}\right]$$

and

$$T(\theta,\theta_0) = \left[\frac{\sin^2\{\pi(Y(\theta)+Y(\theta_0))/2h\} + \sinh^2\{\pi(X(\theta)-X(\theta_0))/2h\}}{\sin^2\{\pi(Y(\theta)-Y(\theta_0))/2h\} + \sinh^2\{\pi(X(\theta)-X(\theta_0))/2h\}}\right]^{1/2}. \tag{A.2}$$

where Gradshteyn & Ryzhik (1981, §1.462) has been used to sum the asymptotic series explicitly. The term $S(\theta,\theta_0)$ is convergent for all θ, θ_0 and its contribution to $K_{mn}^{(e)}$ in (4.10) is given by

$$K_{mn}^{(1)} = \int_0^{2\pi} u_m(\theta_0)\int_0^{2\pi} u_n(\theta)S(\theta,\theta_0)\mathrm{d}\theta\mathrm{d}\theta_0. \tag{A.3}$$

In (A.2), $T(\theta,\theta_0)$ is singular in the denominator at $\theta = \theta_0$ and at $\theta = 0$, $\theta_0 = 2\pi$ and $\theta = 2\pi$, $\theta_0 = 0$ but non-singular in the numerator everywhere. It has the behaviour

$$T(\theta,\theta_0) \sim \frac{2\sin\pi Y(\theta_0)/h}{|\theta-\theta_0|\pi\sigma(\theta_0)}, \qquad \text{as } \theta \to \theta_0. \tag{A.4}$$

$$T(\theta,\theta_0) \sim \frac{2\sin\pi Y(0)/h}{|2\pi \pm (\theta-\theta_0)|\pi\sigma(0)}, \qquad \text{as } \theta - \theta_0 \to \mp 2\pi. \tag{A.5}$$

The singularities now reside in the integral

$$\frac{1}{2\pi}\int_0^{2\pi} u_m(\theta_0)\int_0^{2\pi} u_n(\theta)\ln\left[T(\theta,\theta_0)\right]\mathrm{d}\theta\mathrm{d}\theta_0 = K_{mn}^{(2)} + K_{mn}^{(3)}, \tag{A.6}$$

where we write

$$K_{mn}^{(2)} = \frac{1}{2\pi}\int_0^{2\pi} u_m(\theta_0)\int_0^{2\pi} u_n(\theta)\ln\Big[|\theta-\theta_0|(2\pi+\theta-\theta_0)(2\pi-\theta+\theta_0)T(\theta,\theta_0)\Big]\mathrm{d}\theta\mathrm{d}\theta_0, \tag{A.7}$$

and

$$\begin{aligned} K_{mn}^{(3)} &= -\frac{1}{2\pi}\int_0^{2\pi} u_m(\theta_0)\int_0^{2\pi}\left[u_n(\theta)-u_n(\theta_0)\right]\ln|\theta-\theta_0|(2\pi+\theta-\theta_0)(2\pi-\theta+\theta_0)\mathrm{d}\theta\mathrm{d}\theta_0 \\ &\quad -\frac{1}{2\pi}\int_0^{2\pi} u_n(\theta)u_m(\theta)\left[(2\pi+\theta)\ln(2\pi+\theta)+(4\pi-\theta)\ln(4\pi-\theta)-6\pi\right]\mathrm{d}\theta. \end{aligned} \tag{A.8}$$

Thus, the singularities at $\theta=\theta_0$, $\theta-\theta_0=\pm 2\pi$ have been suppressed by the introduction of the simple logarthmic factor in (A.7) and its reinstatement in (A.8) has been arranged in such a way that the singularities are integrated out analytically. Notice that $K_{mn}^{(3)}$ is in fact independent of all parameters needs to be computed only once, whilst $K_{mn}^{(2)}$ is independent of wavenumber, and needs to be calculated once for each geometrical configuration.

In infinite depth, the kernel H_∞ defined in (5.3) is divided into three parts with the logarithmic singularity exposed explicitly in the first term, labelled $H_\infty^{(s)}$. Thus, only the steps from (A.6) onwards are relevant to infinite depth computations with $T(\theta,\theta_0)=r_0r_1$, where r_0, r_1 are defined in (5.1). In this respect, note the behaviour

$$r_0r_1 \sim 2Y(\theta_0)\sigma(\theta_0)|\theta-\theta_0|, \qquad \text{as } \theta\to\theta_0. \tag{A.9}$$

and

$$r_0r_1 \sim 2Y(0)\sigma(0)|2\pi\pm(\theta-\theta_0)|, \qquad \text{as } \theta-\theta_0\to\mp 2\pi. \tag{A.10}$$

In the case of a thin plate, the parametrisation of the closed boundary, C, of the cylinder in terms of θ where $0\le\theta<2\pi$ is is replaced by the curve L defined in terms of a parameter t, such that the plate extends from tip to tip via $-1\le t\le 1$. Thus we may replace θ and θ_0 by t and t_0 and the limits 0 and 2π by -1 and 1 in (A.1)–(A.4) and (A.6). However the case (A.5) does not come into play since L is not a closed curve, and so (A.7) is replaced simply by

$$K_{mn}^{(2)} = \frac{1}{2\pi}\int_{-1}^{1} u_m(t_0)\int_{-1}^{1} u_n(t)\ln\Big[|t-t_0|T(t,t_0)\Big]\mathrm{d}t\mathrm{d}t_0, \tag{A.11}$$

whilst

$$K_{mn}^{(3)} = -\frac{1}{2\pi}\int_{-1}^{1} u_m(t_0)\int_{-1}^{1} u_n(t)\ln|t-t_0|\mathrm{d}t\mathrm{d}t_0 = (\pi/4n)\delta_{mn}, \qquad n,m\ge 1 \tag{A.12}$$

for the choice of $u_n(t)$ defined by (4.8). This last result can be obtained using Abramowitz & Stegun (1964, equation 22.13.3).

Appendix B. A circular cylinder in infinite depth

First we need to show how the system (4.3) decouples when the submerged cylinder is symmetric about the line $x = 0$. Thus, in terms of the parametric form describing the cylinder, $X(\theta) = -X(2\pi - \theta)$, $Y(\theta) = Y(2\pi - \theta)$, for $0 \le \theta \le \pi$ where $\theta = 0$ is measured vertically downwards from the point $(0, d)$. It is straightforward to use these relations to confirm that $H(\theta|\theta_0) = H(2\pi - \theta|2\pi - \theta_0)$ and $H(\theta|2\pi - \theta_0) = H(2\pi - \theta|\theta_0)$ for either the finite depth case or in infinite depth where we write $H = H_\infty$. Although the details are quite tricky, it can be shown that a consequence of these symmetry relations is

$$K_{2m-1,2n} = K_{2m,2n-1} = 0, \qquad m, n = 1, 2, \ldots$$

where K_{mn} is defined by (4.5). Thus, (4.3) decouples into a pair of systems

$$\sum_{n=1}^{[(N+1)/2]} a_{2n-1} K_{2m-1,2n-1} = F_{2m-1}, \qquad m = 1, \ldots, N, \tag{B.1}$$

and

$$\sum_{n=1}^{N} a_{2n} K_{2m,2n} = F_{2m}. \qquad m = 1, \ldots, N, \tag{B.2}$$

The systems in (B.1) and (B.2) correspond to the components of the solution that are antisymmetric and symmetric (respectively) about $x = 0$.

Further, if the cylinder is circular and described by $X(\theta) = a \sin\theta$, $Y(\theta) = d + a\cos\theta$ then it can be shown that

$$K_{2m,2n} = K_{2m-1,2n-1}, \tag{B.3}$$

and

$$F_{2n} = -\mathrm{i} F_{2n-1}, \tag{B.4}$$

The second relation, (B.4), is easier of the two relations to confirm. First, we write

$$\mathrm{e}^{-KY(\theta)-\mathrm{i}KX(\theta)} = \mathrm{e}^{-Kd}\mathrm{e}^{-Ka\mathrm{e}^{\mathrm{i}\theta}} = \mathrm{e}^{-Kd}\sum_{r=0}^{\infty}\frac{(-Ka)^r}{r!}\mathrm{e}^{\mathrm{i}r\theta}. \tag{B.5}$$

Then

$$F_{2n} = \mathrm{i}\int_0^{2\pi} \mathrm{e}^{-KY(\theta)-\mathrm{i}KX(\theta)} \cos n\theta \mathrm{d}\theta = \mathrm{i}\pi \mathrm{e}^{-Kd}(-Ka)^n/n!, \tag{B.6}$$

using (B.5) and similarly

$$F_{2n-1} = -\pi \mathrm{e}^{-Kd}(-Ka)^n/n!, \tag{B.7}$$

whence (B.4) follows.

Establishing the relation (B.3) is slightly more awkward. The complication is attached to the component $K_{mn}^{(s)}$ of K_{mn} containing the singular part of the kernel, $H_\infty^{(s)}$, although (B.5) can be used in a similar manner to above to show (B.3) holds for the individual components $K_{mn}^{(r)}$ and $K_{mn}^{(i)}$. We omit the rather lengthy details here and simply state the result in a form which exposes the different components that make up K_{mn}:

$$K_{2m,2n} = K_{2m-1,2n-1} \;=\; \frac{\pi\delta_{mn}}{2m} + \frac{\pi}{2(n!m!)}\int_0^\infty (-\nu a)^{m+n-1}\mathrm{e}^{-2\nu d}\mathrm{d}\nu$$

$$+\frac{\pi}{n!m!}\int_0^\infty \frac{(-\nu a)^{m+n}}{K-\nu}\mathrm{e}^{-2\nu d}\mathrm{d}\nu - \mathrm{i}\pi^2\frac{(-Ka)^{m+n}}{n!m!}\mathrm{e}^{-2Kd}$$

$$= \frac{\pi\delta_{mn}}{2m} + \frac{\pi(-Ka)^{m+n}}{2(n!m!)}\int_0^\infty \frac{1+t}{1-t}t^{m+n-1}\mathrm{e}^{-2Kdt}\mathrm{d}t - \mathrm{i}\pi^2\frac{(-Ka)^{m+n}}{n!m!}\mathrm{e}^{-2Kd} \qquad \text{(B.8)}$$

where δ_{mn} is the Kronecker delta.

Remarkably, the systems (B.1) and (B.2) with (B.6) (B.7) and (B.8) are identical to the systems of equations one would derive for the antisymmetric and symmetric components of the solution to the scattering by a submerged horizontal cylinder in infinite depth if one were to use the multipole method (c.f. Ursell (1950). Also see Evans *et al* (1979)).

Using (B.6) and (B.7) in (B.1) and (B.2) implies that the coefficients are also related pairwise by

$$a_{2n} = -\mathrm{i}a_{2n-1}, \qquad n = 1, \ldots, N. \qquad \text{(B.9)}$$

Using with (4.6), with the factor $1/(2kh)$ ommitted since we are dealing with the infinite depth case, gives

$$\tilde{R} = \mathrm{i}\left[\sum_{n=1}^{N} a_{2n-1}F_{2n-1}^{(1)} + \sum_{n=1}^{N} a_{2n}F_{2n}^{(1)}\right] = 0$$

from (B.4) and (B.9).

References

[1] Abramowitz, M.A. & Stegun, I. 1965 *Handbook of Mathematical Functions.* Dover.

[2] Davies, A. & Leppington, F.G. 1985 Scattering of long surface waves by circular cylinders or spheres. *Quart. J. Mech. Appl. Maths.,* **38**, 411–432.

[3] Dean, W.R. 1945 On the reflexion of surface waves by a flat plate floating vertically. *Proc. Camb. Phil. Soc.,* **41**, 231–238.

[4] Dean, W.R. 1948 On the reflexion of surface waves by a submerged circular cylinder. *Proc. Camb. Phil. Soc.,* **44**, 483–491.

[5] Evans, D.V. 1970 Diffraction of surface waves by a submerged vertical plate. *J. Fluid Mech.,* **40**, 433–451.

[6] Evans, D.V., Jeffery, D.C., Salter, S.H. & Taylor, J.R.M. 1979 Submerged cylinder wave energy device: theory and experiment. *Appl. Ocean. Res.,* **1**, 3–12.

[7] Fernyhough, M. 1994 Applications of the Residue and Modified Residue Calculus Method in linear acoustic and water wave theory. Ph.D. Thesis, University of Bristol, UK.

[8] Gradshteyn, I.S. & Ryzhik, I.M. 1981 *Tables of Integrals, Series and Products.* New York: Academic Press.

[9] Grue, J. & Palm, E. 1984 Reflection of surface waves by submerged cylinders. *Appl. Ocean Res.,* **6**, 54–60.

[10] Leppington, F.G. & Siew, P.F. 1980 Scattering of surface waves by a submerged circular cylinder. *Appl. Ocean Res.,* **2**, 129–137.

[11] McIver, M. 1985 Diffraction of water waves by a moored, horizontal, flat plate. *J. Engng. Math.,* **8**, 279–301.

[12] Mei, C.C. 1983 The Applied Dynamics of Ocean Surface Waves. Wiley-Interscience.

[13] Newman, J.N. 1966 Propataion of waves over long two-dimensional obstacles. *J. Fluid Mech.,* **23**, 23–29.

[14] McIver, M. & Urka, U. 1995 Wave scattering by circular arc shaped plates. *J. Engng. Math.* **29**(6), 575–589.

[15] Ogilvie, T.F. 1963 First- and second-order forces on a cylinder submerged under a free surface. *J. Fluid Mech.,* **16**, 451–472.

[16] Parsons, N. & Martin. P. 1992 Scattering of water waves by submerged plates using hypersingular integral equations. *Appl. Ocean Res.,* **14**, 313–321.

[17] Parsons, N. & Martin. P. 1994 Scattering of water waves by submerged curved plates and by surface-piercing plates. *Appl. Ocean Res.,* **16**, 129–139.

[18] Patarapanich, M. 1984 Forces and moments on a horizontal plate due to wave scattering. *Coastal Engng.,* **8**, 279–301.

[19] Porter, R. 2001 Trapping of water waves by pairs of submerged cylinders. *(submitted for publication)*

[20] Porter, R. & Evans, D.V. 1995 Complementary approximations to wave scattering by vertical barriers. *J. Fluid Mech.,* **294**, 155–180.

[21] Porter, R. & Porter, D. 2000 Water wave scattering by a step of arbitrary profile. *J. Fluid. Mech.,* **411**, 131–164.

[22] Staziker, D.J., Porter, D. & Stirling, D.S.G. 1996 The scattering of surface waves by local bed elevations. *Appl. Ocean Res.,* **18**, 283–291.

[23] Ursell, F. 1950 Surface waves on deep water in the presence of a submerged circular cylinder. *Proc. Camb. Phil. Soc.,* **46**, 141–158.

[24] Vada, T. 1987 A numerical solution of the second-order wave-diffraction problem for a submerged cylinder of arbitrary shape. *J. Fluid Mech.,* **174**, 23–37.

[25] Wehausen, J.V. & Laitone, E.V. 1960 Surface waves, *Handbuch der Physik.* Vol IX. Berlin: Springer-Verlag.

[26] Yu, Y.S. & Ursell, F. 1961 Surface waves generated by an oscillating circular cylinder on water of finite depth: theory and experiment. *J. Fluid Mech.,* **11**, 529–511.